

NUCLEAR RESONANCE SCATTERING AND MÖSSBAÜER EFFECT

A Graduate Project Submitted to the School of Graduate
Studies of Addis Ababa University



In partial Fulfillment of the Requirements for the degree of Masters of
Science in Physics

BY
MESSELE KEBEDE

July 2010
Addis Ababa
Ethiopia

ADDIS ABABA UNIVERSITY SCHOOL OF GRADUATE
STUDIES

NUCLEAR RESONANCE SCATTERING AND MÖSSBAÜER
EFFECT

BY

MESSELE KEBEDE

DEPARTMENT OF PHYSICS FACULTY OF SCIENCE

Approved by the Examination Committee

Name

Signature

Professor A.K. Chaubey

Advisor

Dr. Tilahun Tesfaye

Examiner

| Contents | page |
|--|------|
| List of figures..... | i |
| List of tables..... | ii |
| Acknowledgement | iii |
| Abstract | iv |
| Chapter 1 | 1 |
| Introduction | |
| Chapter 2 | 6 |
| The Mössbauer Effect | |
| 2.1 Resonant Scattering of γ -Rays..... | 6 |
| 2.2 Compensation for Recoil Energy | 10 |
| 2.3 The Discovery of the Mössbauer Effect | 11 |
| 2.4 The Mössbauer Spectrum | 15 |
| 2.4.1 The Measurement of a Mössbauer Spectrum | 15 |
| 2.4.2 The Shape and Intensity of a Spectral Line | 16 |
| 2.5 Mössbauer isotopes | 22 |
| 2.6 Mössbauer parameters | 25 |
| 2.7 Importance of Mössbauer's discovery | 32 |
| Chapter 3 | 33 |
| Some applications of Mössbauer effect | |
| 3.1 Mössbauer effect to General relativity..... | 33 |
| 3.1.1 Experiment | 36 |
| 3.2 Mössbauer effect in Dy_2O_2S | 38 |
| 3.2.1 Introduction | 38 |
| 3.2.2 Experiment and conclusion | 38 |
| Conclusion | 43 |
| References..... | 46 |

List of figures

| | | |
|-----------------|--|----|
| Fig 1.1 | Gamma emission and absorption lines of isolated nuclei, R is the energy shift produced by the recoil effect E_r is the resonance energy, and δ is the Doppler width | 4 |
| Fig1.2 | Emission and absorption in atomic and nuclear system | 5 |
| Fig1.3 | Recoil momentum obtained by the stationary emitter and absorber consequent on the emission and absorption of a photon | 5 |
| Fig2.1 | Schematic diagram of resonance scattering systems | 7 |
| Fig2.2 | Recoil of a nucleus after emitting a gamma ray | 7 |
| Fig2.3 | Emission and absorption gamma ray spectra when recoil present | 8 |
| Fig2.4 | Decay scheme of ^{191}Os | 11 |
| Fig2.5 | Resonance absorption curve of the 129 Kev gamma rays by ^{191}Ir | 12 |
| Fig2.6 | Emission and absorption spectra of gamma rays when $E_R \ll \hbar\omega$ | 13 |
| Fig2.7 | Measuring a Mössbauer spectrum | 15 |
| Fig2.8 | $\epsilon(v_r)/f_s$ as a function of t_a for $\xi=0.7, 1.0, \text{ and } 1.3$ | 19 |
| Fig2.9 | Contributions to the Mössbauer spectrum in transmission geometry | 21 |
| Fig2.10 | $A(t_a)$ as a function of t_a . In plotting this curve, the proportionality constant ($f_s\Gamma_a\Pi$) in eq(2.29) is taken to be 1 | 22 |
| Fig2.11 | Magnetic splitting with and without quadrupole interaction for ^{57}Fe | 28 |
| Fig2.12 | The anti ferromagnetic structure of Mno | 29 |
| Fig2.13 | Representation of main Mössbauer parameters for the $I=3/2 \rightarrow 1/2$ transition $E \approx E_\gamma$ | 31 |
| Fig3.1 | Rigid rod AB has constant acceleration a in inertial frame | 34 |
| Fig3.2 | Simplified diagram of experimental arrangement for determining red shift.... | 37 |
| Fig3.3 | Magnetic structure of Dy_2O_3 as determined by neutron diffraction measurements..... | 39 |
| Fig3.4 | Mössbauer spectrum of Dy_2O_3 single crystal, exhibiting the disappearance of the $\Delta m=0$ lines | 41 |
| Fig3.5 a,b,c,d- | Mössbauer spectra of Dy_2O_3 power sample at different temperatures. | |
| Figure 3.5d | is a computer fit | 41 |

List of tables

| | | |
|----------|---|----|
| Table2.1 | Comparison between photon emission from the ^{57}Fe nucleus and the Na atom while each decays from its first excited state to the ground state | 9 |
| Table2.2 | Nuclear parameters for selected Mössbauer transition | 24 |

Acknowledgement

First and for most I praise the almighty God for this goodness and that mercy that me to be alive .

My deepest heart felt thanks goes to my work advisor and instructor professor A.K.Chaubey for this sound advise and suggestion he gave me through out all my steps to the completion of this work.

In addition to this ,I thank my wonderful family for their continued patience and understanding the completion of this enormous task would not have been possible with out their endless love and faith in me.

Finally, I would like to dedicate this work to my family.

Abstract

The resonance scattering of a gamma rays constitutes the nuclear analogue to the well-known optical fluorescence effect .Since then several methods have been developed which led to the observation of resonance scattering or absorption in a number of first excited nuclear states. A major break through took place in 1958 when the phenomenon of recoilless nuclear resonance absorption was discovered . This new absorption effect provided a means for the elimination of the energy losses by recoil , these being the most serious obstacle for the observation of nuclear resonance absorption or scattering .Simultaneously gamma lines of utmost narrowness became available .It is this particular feature which opened wide range of applications for new effect , in such fields as nuclear physics ,solid state physics, and relativity, and made possible investigations which could not even be considered only a few years ago.

CHAPTER 1

INTRODUCTION

With the emission of characteristic line spectra by atoms, it was but natural to expect resonance in atomic system and indeed Lord Rayleigh (1894) at the end of the last century predicted that resonance scattering should occur in atomic systems. However it was only in 1904, R.W. Wood (1934) demonstrated the phenomenon of resonance fluorescence in atomic systems by a simple experiment.

In the early stages, the explanation of resonance fluorescence in atomic systems was based on mechanical analogies. The oscillators in the absorbing system were supposed to be exactly in tune with the frequency incoming radiation. Although this mechanical picture could satisfactorily explain some features of resonance fluorescence, it predicted a definite phase relationship between the incoming and the scattered radiation.

With the advent of Bohr's theory (Bohr, 1913), for according to this theory, the emission and absorption of light in the form of photons was supposed to be a consequence of the transition of an atom from an excited state having energy E_1 to the ground state having an energy E_0 and vice versa respectively such that $E_1 - E_0 = h\nu$, where h is the Planck's constant and ν frequency of radiation. It is thus easy to see that when the sodium atom is excited, it emits photons corresponding to definite frequencies and hence energies. When these photons strike absorbing atoms they are absorbed raising the atoms from the ground state to an excited state where they remain for a very short time (life time of the excited state) after which the absorbing atoms return to the ground state with an emission of radiation of the same frequency in all directions (as shown in Fig 1.2).

Thus the intensity of the incoming radiation is decreased along the direction joining the emitter and the absorber but increased along any other direction. This mechanism predicted that the primary and secondary radiations from the same atomic system should have the same wavelength and that absorption and emission are independent processes such that no phase relation should exist between the primary and the scattered radiations. With the satisfactory explanation of the salient features of the phenomenon of resonance fluorescence, finer aspects of the characteristics of radiation emitted by an

atom such as the line width ,coherence ,radiation damping ,etc.

The observation of gamma rays with sharply defined frequencies emitted by nuclei either spontaneously or after excitation by one of the several processes ,revealed that nuclei can exist in excited state ,the energies of which can be determined from Bohr's relation $E_1-E_0= h\nu$, just as in the case of atomic systems .It was ,therefore ,merely an extension of the argument given for the observation of resonance fluorescence in atomic systems to ask whether it would be possible to observe resonance fluorescence of gamma rays .Indeed a systematic search started with the experiments of Kuhn in 1929 .Several unsuccessful attempts were made since the early experiments of Kuhn (1929)but it was in 1957 that Mössbauer demonstrated the feasibility of the absorbing resonance fluorescence of gamma rays by embedding the absorbing and emitting nuclei in well bound crystalline solids. In order to appreciate the difficulties in observing resonance fluorescence of gamma rays and at the same time the importance of Mössbauer's discovery ,it is necessary to look more closely into the process of resonance fluorescence .

If the mass of the emitting system which was supposed to be at rest before emission is m ,then the recoil momentum necessitates that the emitting system should receive an energy which may be called the recoil energy R is given by

$$R = \frac{p^2}{2m} \quad (1.1)$$

This energy is obviously obtained from the de-excitation energy of the emitting system .Thus it is easy to see from the point of view of conservation of energy ,that the emitted a photon should have energy less than the de-excitation energy of the emitting system .This means that the photon energy will be less or in other words there will be a shift towards the red end of the spectrum when the emitting system ,either the atomic or the nuclear ,recoils .

Let us determine the change in the energy of the photon due to the recoil of the emitting system .Such a quantum mechanical system de-excites itself from an excited state E_1 to the ground state E_0 by the emission of a photon .If all the transition energy (E_1-E_0) were

to go into the photon ,then its frequency would be given by $(E_1-E_0)=h\nu$. The emitted line in this case will be centered at (E_1-E_0) on the energy scale (as shown Fig1.3).

However, it is known that a photon ,a quantum of an electromagnetic field has a momentum $\mathbf{p}=h\nu/c$ along the direction of propagation .As stated earlier,the emitting system ,be it an atom or a nucleus ,will recoil in a direction opposite to the direction of the emission of a photon and get a recoil momentum \mathbf{p} equal to the momentum of the photon .The kinetic energy which the emitting system acquires as a consequence of this recoil will be given by

$$R = \frac{p^2}{2m} = \frac{h^2 \nu^2}{2mc^2} \quad (1.2)$$

Where m mass of the emitting system

It may be noted that the recoil energy R is proportional to the square of the photon energy and is, therefore ,much larger for gamma ray emission (with energy ranging from few KeV to few MeV) as compared to the emission of an optical photon which has energies ranging between 1-10eV .Indeed the recoil suffered by the nucleus during gamma emission is some 10^6 to 10^{12} times the recoil suffered by an atom during the emission of a photon in the visible range .For example , mercury atom obtains a recoil energy of 0.0647×10^{-9} eV during the emission of its principle radiation $\nu=1183 \times 10^{12}$ cps,where as Hg^{198} nucleus obtains a recoil energy of 0.067eV during the emission of γ — ray of energy 158×10^3 eV.

The recoil energy of the emitting system is obviously obtained from the transition energy and ,therefore, we have

$$(E_1-E_0)=h\nu+R \quad (1.3)$$

In this situation the photon has an energy slightly less than the transition energy .The emission line is no more centered at (E_1-E_0) but centered at $[(E_1-E_0)-R]$, i.e it is slightly shifted to words the red end of the spectrum .Again to take the same example ,consequent on the recoil suffered by the mercury atom ,the principle radiation is shifted by 0.5×10^{-6} wave number where as the gamma ray from Hg^{198} shifts by 539.99 wave number .

Essentially similar thing happen during the absorption of a photon by an atom or nucleus. Thus when a photon corresponding to the transition energy (E_1-E_0) is incident on absorbing atom or the nucleus ,then the incoming photon is absorbed .During the process of absorption ,the photon momentum is it were reduced to zero and hence to conserve the momentum the absorbing system recoils and obtains a momentum p ,along the direction of the incoming photon .Consequent on this recoil ,the absorbing system

acquires an energy $R = \frac{p^2}{2m} = \frac{h^2 \nu^2}{2mc^2}$.This kinetic energy has necessarily to be supplied by the incoming photon .Thus to excite the absorbing system from the ground state E_0 to the excited E_1 it is not enough to have an energy (E_1-E_0)but the photon must have an energy $[(E_1-E_0)+R]$.In other words ,the absorption line is not centered at (E_1-E_0) but is located at $[(E_1-E_0)+R]$.The shift of the absorption line towards the violet end of the spectrum is equal to the shift of the emission line towards the red end of the spectrum .Indeed the two separated on the energy scale by $2R$.This implies that the system has maximum emission corresponding to the energy (E_1-E_0-R) and maximum absorption corresponding to the energy (E_1-E_0+R) apparently violating Kirchoff's law.

It is thus seen that the absorption line does not overlap the emission line ,because of the recoil obtained by the emitting and absorbing systems during the emission and absorption processes respectively ¹.

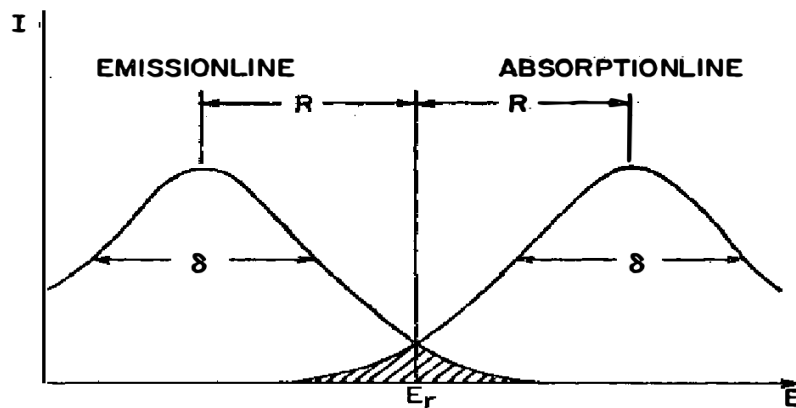


Fig 1.1 Gamma emission and absorption lines of isolated nuclei , R is the energy shift produced by the recoil effect E_r is the resonance energy ,and δ is the Doppler width ¹¹ .

Indeed, no resonance fluorescence should be observed even in the visible part of the

spectrum emitted by atomic systems unless some other fortunate circumstances make it possible for the emission line and absorption to overlap, at least partially ¹.

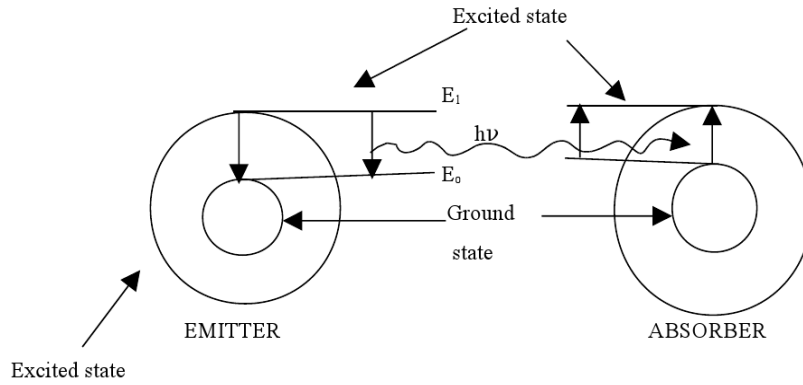


Fig.1. 2. Emission and absorption in atomic and nuclear systems

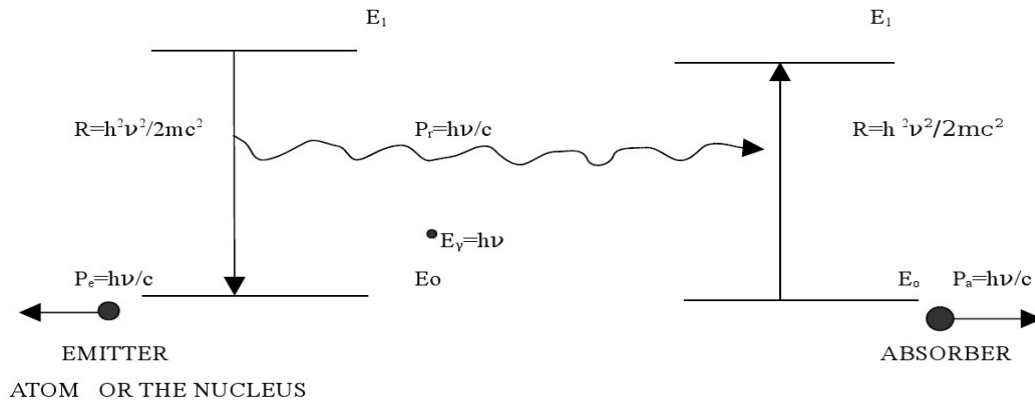


Fig 1.3 Recoil momentum obtained by the stationary emitter and absorber consequent on the emission and absorption of a photon

CHAPTER 2

The Mössbauer Effect

2.1 Resonant Scattering of γ -Rays

It was at the beginning of the 20th century that resonant scattering of light became experimentally verified. For example, when a beam of yellow light (the D-lines) from a sodium lamp goes through a flask with low-pressure sodium vapor in it, sodium atoms in the 2S ground state will have a relatively large probability of absorbing the incident photons and making a transition to the excited 2P state (as shown in Fig. 2.1). When these atoms return to the ground state, they emit a yellow light of the same wavelength (known as resonance fluorescence) in all spatial directions. In the original direction of the incident beam, the light intensity will be substantially reduced. This phenomenon can be considered as a process of resonant scattering of photons.

In 1929, Kuhn pointed out that a similar gamma ray resonant scattering phenomenon should also exist for the nuclei. However, research during the next twenty plus years failed to produce satisfactory experimental results to support his predictions. The reason was quite clear. Because of the law of momentum conservation, after emitting a gamma ray, the nucleus obtains a velocity in the opposite direction (recoil). Compared to the recoil velocity of an atom when the atom emits a visible photon, the nucleus recoils with a velocity several orders of magnitude larger, takes enough energy away from the emitted γ - ray, and prevents the observation of resonance absorption. We will now discuss this in detail.

Suppose a free nucleus of mass M and initial velocity v is in the excited state E_e , emitting a γ - ray in the x -direction when it returns to the ground state. Figure 2.2 shows the energy levels and recoil of the nucleus, where v_x is the x -component of the initial velocity and v_R its recoil velocity (relative to v_x). According to momentum conservation and energy conservation, we have

$$Mv_x = \frac{E_\gamma}{c} + M(v_x - v_R)$$
$$E_e + \frac{1}{2}Mv_x^2 = E_g + E_\gamma + \frac{1}{2}M(v_x - v_R)^2 \quad (2.1)$$

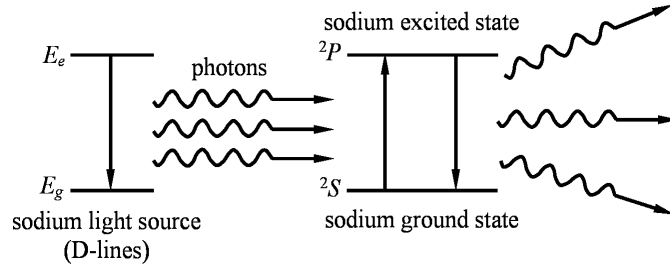


Fig. 2.1 Schematic diagram of resonance scattering of light.

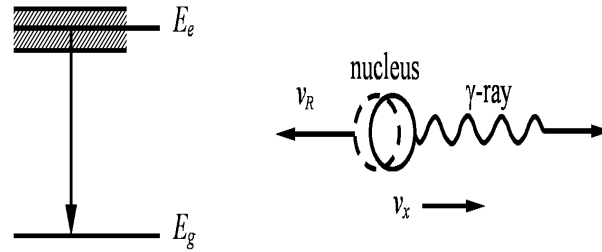


Fig. 2.2 Recoil of a nucleus after emitting a gamma ray.

where E_g is the ground state energy of the nucleus and E_e is the energy of the excited state. From the above equations, we obtain

$$E_\gamma = (E_e - E_g) - \frac{1}{2} M v_R^2 + M v_x v_R = E_0 - E_R + E_D \quad (2.2)$$

where E_0 is the energy difference between the excited state and the ground state

$$E_0 = E_e - E_g \quad (2.3)$$

E_R is the recoil energy

$$E_R = \frac{1}{2} M v_R^2 = \frac{E_\gamma^2}{2Mc^2} \quad (2.4)$$

and E_D depends on the initial velocity v_x and is due to the Doppler effect (known as the Doppler energy shift)

$$E_D = M v_x v_R = \frac{v_x}{c} E_\gamma \quad (2.5)$$

We will now consider the following two cases ($v_x = 0$ and $v_x \neq 0$) separately.

(a) If $v_x = 0$, then $E_D = 0$. In this case, the excited nucleus is at rest. The energy spectrum of the emitted gamma rays from such nuclei is shown by the dashed line in Fig. 2.3. The spectrum is a sharp peak centered at $E_0 - E_R$, and its width at

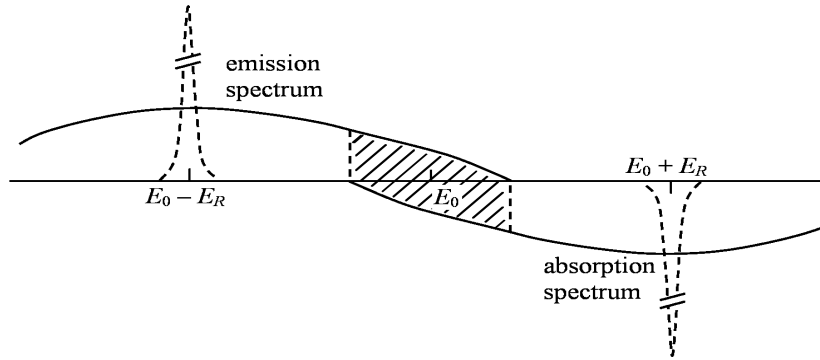


Fig. 2.3 Emission and absorption gamma ray spectra when recoil is present.

the half height is nearly the same as the natural width Γ_n of the excited energy level.

The nuclei in the ground state (E_g) may resonantly absorb the incident gamma rays and transit to the excited state E_e . The energy distribution of these absorbed gamma rays is identical to the emission spectrum, except for a shift of E_R to the right of E_0 , as shown in Fig. 2.3. The energy difference between the emitted and the absorbed gamma rays is $2E_R$. Therefore, the fundamental condition necessary for the photon's resonant scattering is

$$\frac{\Gamma_n}{2E_R} > 1 \quad (2.6)$$

that is, the recoil energy must be less than half of the natural width of the excited state. Comparing the data for the ^{57}Fe nucleus and the sodium atom in Table 2.1, we can easily see that for the Na atom, condition (2.6) is completely satisfied, because the emission spectrum and the absorption spectrum are almost overlapping, resulting in

very large probability for resonant absorption. For the ^{57}Fe nucleus, however, its value is far from satisfying condition (2.6). Although the natural widths Γ_n of a nucleus and an atom are comparable, the former gives a much more energetic photon than the latter, usually by three orders of magnitude.

Table 2.1 Comparison between photon emissions from the ^{57}Fe nucleus and the Na atom while each decays from its first excited state to the ground state

| | E_γ | $\Gamma_n(\text{ev})$ | $E_R(\text{ev})$ | $\Gamma_n/2E_R$ |
|--------------------------|--------------------|-----------------------|-----------------------|----------------------|
| nucleus ^{57}Fe | 14.4×10^3 | 4.65×10^{-9} | 1.95×10^{-3} | 1.2×10^{-6} |
| Na atom (D-lines) | 2.1 | 4.39×10^{-8} | 1.0×10^{-10} | 2.2×10^2 |

This makes their E_R values differ by more than six orders of magnitude, and this is the reason why resonant absorption of gamma rays is usually not observed.

(b) For $v_x \neq 0$, the situation is more common. Because of the random thermal motions of free atoms, their velocities v_x may have large variations, described by the Maxwell distribution

$$p(v_x)dv_x = \left(\frac{M}{2\pi k_B T} \right)^{1/2} \exp\left(-\frac{M}{2k_B T} v_x^2 \right) dv_x$$

where k_B is Boltzmann's constant and T is the absolute temperature. This distribution will greatly broaden the emission spectrum (or the absorption spectrum), as indicated by the solid line in Fig. 2.3. This broadening is due to the Doppler effect, and hence is known as Doppler broadening. Since the width of the above velocity distribution is $2(2k_B T \ln 2/M)^{1/2}$, the width of the emission spectral line is then

$$\Delta E_D = Mv_R \left(2\sqrt{\frac{2k_B T \ln 2}{M}} \right) = 4\sqrt{E_R k_B T \ln 2} \quad (2.7)$$

For ^{57}Fe at $T = 300 \text{ K}$, $\Delta E_D = 2.4 \times 10^{-2} \text{ eV} > 2E_R$. This means that the emission spectrum partially overlaps the absorption spectrum (the shaded region in Fig.2.3), and it may be possible to observe some effect of resonant absorption.

2.2 Compensation for Recoil Energy

As discussed above, if the nucleus is free to move, the lost energy due to recoil must be compensated before substantial resonance absorption of γ -rays can be observed. Several ingenious experiments were devised to achieve this compensation, two of which are briefly explained here.

The first experiment made use of mechanical motion of the source. The radioactive source was mounted on the tip of a high-speed rotor. Due to the Doppler effect, the γ -

rays acquired an additional energy ΔE ,
$$\Delta E = \frac{v}{c} E_\gamma \quad (2.8)$$

It was possible to adjust the speed v of the rotor to completely compensate the recoil

energy loss, i.e. $\left(\frac{v}{c}\right) E_\gamma = 2 E_R$ (for ^{57}Fe , $v = 81 \text{ m s}^{-1}$). This experiment had two problems. First, only during a very short portion of the rotation period could the emitted γ -rays be used in the experiment, and thus the source was largely under-utilized. Second, the experiment was limited by the maximum obtainable speed of the mechanical rotor and especially by the poor stability of the rotor speed.

The second experiment used the fact described in Eq. (2.7) that the Doppler broadening is increased by raising the temperature. As a result, it would cause increases in the overlapping region in Fig. 2.3, and therefore increases in the probability of resonance absorption.

By the above means, the phenomenon of gamma ray resonant absorption had been observed before 1954 but a major shortcoming was that these resonance absorption experiments all involved recoil, which would never be practically significant due to low γ -ray counts and poor energy resolution. A historic discovery by Mössbauer of resonant absorption without recoil completely eliminated the need for the above effort to compensate the energy loss. We will now describe this discovery.

2.3 The Discovery of the Mössbauer Effect

In 1958, Rudolf L. Mössbauer was investigating the resonant absorption of the 129 keV γ – ray in ^{191}Ir nucleus and discovered that if the source nuclei ^{191}Os and absorber nuclei ^{191}Ir were rigidly bound in crystal lattices, the recoil could be effectively eliminated and the resonant absorption was readily observed.

In a crystal lattice, an atom is held in its equilibrium position by strong chemical bonds corresponding to an energy of typically 10 eV. For the 129 keV transition in free ^{191}Ir nucleus (Fig. 2.4), the recoil energy is 4.7×10^{-7} eV, much smaller than the chemical bond energy. Therefore, from the classical view-point, when the γ – ray is emitted by a nucleus bound in a lattice, the nucleus will not recoil alone, but the entire crystal lattice recoils together (a total of about 10^{18} atoms). In this case, the mass M in the denominator of Eq. (2.4) should be the mass of the whole crystal, not the individual nucleus. This reduces the recoil energy to a negligible amount ($\sim 10^{-20}$ eV). Consequently, Eq. (2.6) is satisfied, Eq. (2.2) is simplified to $E_\gamma = E_o$, and the entire process becomes a recoilless resonant absorption.

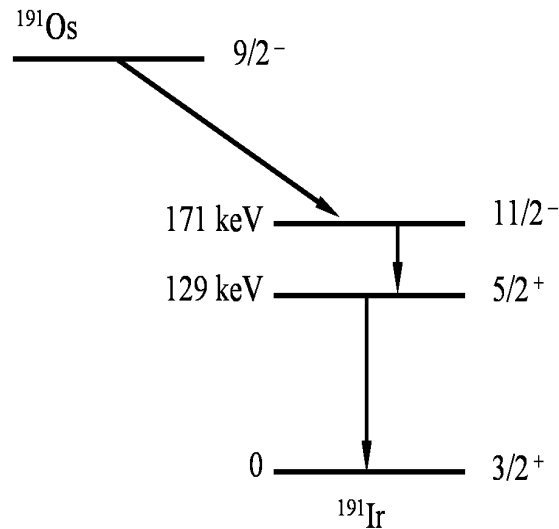


Fig. 2.4 Decay scheme of ^{191}Os .

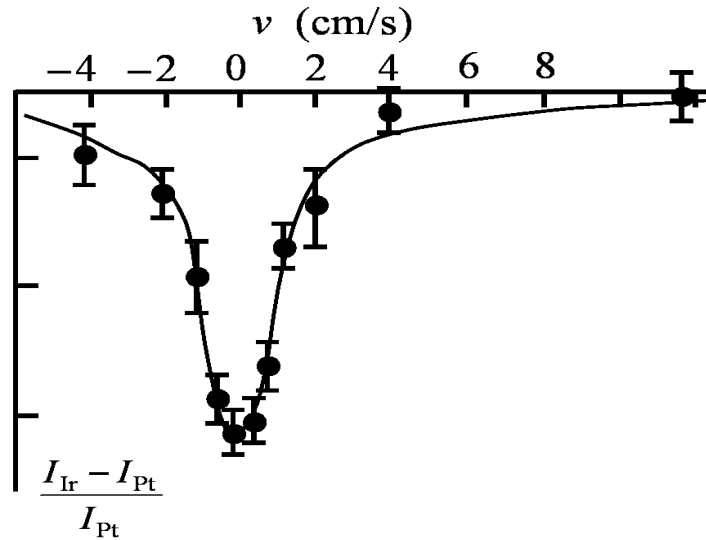


Fig. 2.5 Resonance absorption curve of the 129 keV γ – rays by ^{191}Ir .

In Mössbauer’s first experiment where he observed recoilless resonance absorption of γ – rays, the radiation source was a crystal containing ^{191}Os and the absorber was an iridium crystal, both at a temperature of 88 K. A platinum (Pt) comparison absorber of the same thickness was used to measure the background. Because the process was recoilless, the Doppler velocity only needed to be small, about several centimeters per second. The results from that first experiment are reproduced in Fig. 2.5, where the horizontal axis represents the γ – ray energy variation ΔE (or source velocity v). When the source is moving towards the absorber, $v > 0$, and when the source is moving away from the absorber, $v < 0$. The vertical axis represents the relative change in the γ – ray intensity, $(I_{\text{Ir}} - I_{\text{Pt}})/I_{\text{Pt}}$, where I_{Ir} and I_{Pt} are the γ – ray intensities transmitted through the Ir and Pt absorbers, respectively.

As shown in Fig. 2.5 and pointed out by Mössbauer, the width of the spectrum is 4.6×10^{-6} eV, which is just slightly more than twice the natural width of the 129 keV energy level of ^{191}Ir . Never before had such a high resolution in energy ($\Delta E/E \approx 3.5 \times 10^{-11}$) been achieved, and Mössbauer’s research results were fundamentally different from what anyone had previously obtained from γ – ray resonant scattering, because he observed γ – ray emission and absorption events in which the recoil was completely absent. Not too long after the discovery of recoilless γ – ray emission and resonant

absorption, this effect was named after its discoverer and is now known as the Mössbauer effect.

In reality, the Mössbauer nucleus is not rigidly bound, but is usually free to vibrate about its equilibrium position. Photons may exchange energy with the lattice, resulting in the creation or annihilation of quanta (phonons) of lattice vibrations. Suppose we have an Einstein solid with one vibrational frequency ω , then the lattice can only receive or release energies in integral multiples of $\hbar\omega$ ($0, \pm\hbar\omega, \pm 2\hbar\omega, \dots$). So if $E_R < \hbar\omega$, the lattice cannot absorb the recoil energy, i.e., the zero phonon process, and the γ -ray is emitted without recoil. The probability of having such a process is known as the recoilless fraction f , an extremely important parameter in Mössbauer spectroscopy.

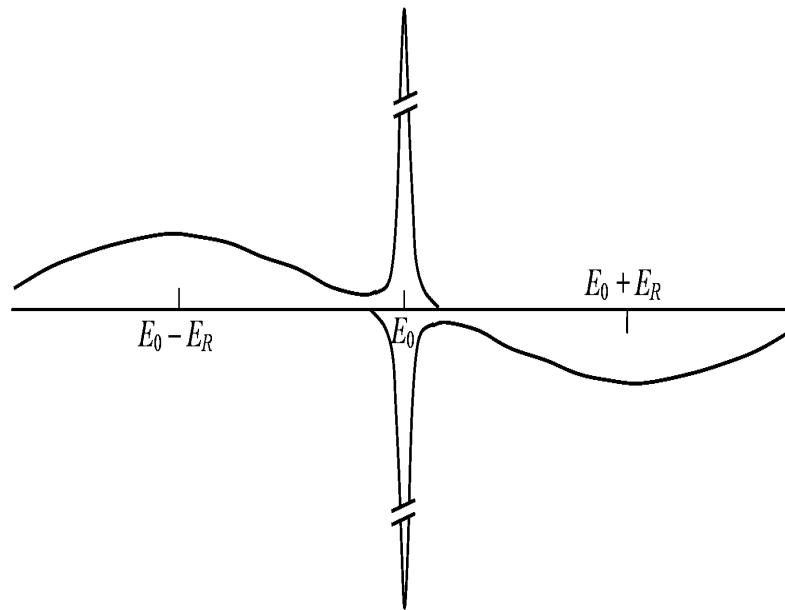


Fig. 2.6 Emission and absorption spectra of γ -rays when $E_R \ll \hbar\omega$.

In a typical lattice, both E_R and $\hbar\omega$ are in the ranges 10^{-3} to 10^{-1} eV. Obviously, the value of f depends on how E_R compares with $\hbar\omega$. Only when $E_R \ll \hbar\omega$ will f be reasonably large (see Fig. 2.6). According to Lipkin's sum rule, when a large number of absorption events are considered, the average energy transferred to the lattice must be

exactly equal to E_R .

Let a total of m γ – photons with E_γ be absorbed among which n of them cause zero phonon creation and the rest($m - n$) photons each excites a single phonon (neglecting double phonons), then

$$mE_R = (m - n)\hbar\omega$$

Based on the Einstein model, we arrive at an approximate expression for the recoilless fraction

$$f = \frac{n}{m} = 1 - \frac{E_R}{\hbar\omega} \quad (2.9)$$

It can be seen from this expression that, in order to observe the Mössbauer effect, the recoilless fraction f should be sufficiently large, and we would like to have the following condition between E_R and $\hbar\omega$:

$$E_R \ll \hbar\omega \quad (2.10)$$

A more precise expression for the recoilless fraction is

$$f = e^{-k^2 \langle x^2 \rangle}$$

where $\langle x^2 \rangle$ is the mean square displacement of a nucleus along the direction of the wave vector \mathbf{k} of the emitted γ – ray. This expression points out that in a liquid or a gas, the Mössbauer effect is extremely difficult to observe because of the large $\langle x^2 \rangle$ values. Also, a small \mathbf{k} value would give a large f value, and therefore γ – rays with lower energies will favor the observation of the Mössbauer effect. At present, the Mössbauer effect has been observed from more than 100 nuclear isotopes (e.g., ^{57}Fe , ^{119}Sn , ^{191}Ir , etc.), among which one of the highest γ – ray energies is 187 keV in ^{190}Os . For a γ – ray energy higher than 100 keV, the source and the absorber are usually kept at low temperatures to reduce their $\langle x^2 \rangle$ values.

2.4 The Mössbauer Spectrum

2.4.1 The Measurement of a Mössbauer Spectrum

The shape of a resonance curve is often used to characterize the properties of the resonance system. For example, we can obtain the natural width Γ_n of the excited energy state from the line width of the measured γ -ray resonance curve and estimate the life time of the energy state according to the uncertainty relation $\tau \Gamma_n \sim \hbar$. A Mössbauer spectrum is a recoil-free resonance curve. To measure this, we no longer need those high-speed rotors, but it is still necessary to use the Doppler effect for modulating the γ -ray energy E_γ within a small energy range, $E_\gamma(1 \pm \frac{v}{c})$. A velocity transducer with the mounted source moves with respect to the absorber and the emitted γ -ray energy is therefore modulated, as shown in Fig. 2.7. A Mössbauer absorption spectrum, shown on the right of Fig. 2.7, is a record of transmitted γ -ray counts through the absorber as a function of γ -ray energy, whose line width has a minimum value of $\Gamma_s + \Gamma_a$ (the sum of the natural widths of the Mössbauer nuclei in the source and the absorber).

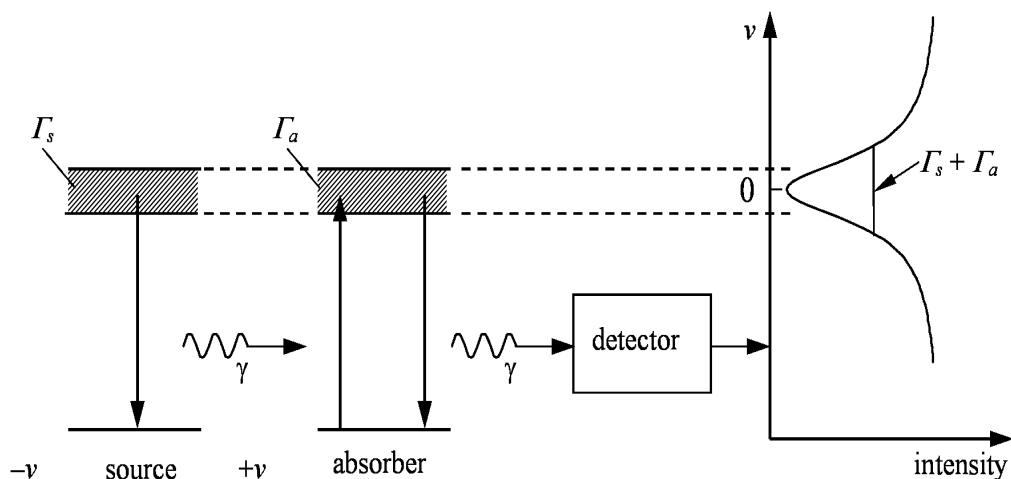


Fig. 2.7 Measuring a Mössbauer spectrum.

For the sake of simplicity, it is customary to use the source velocity (in mm s^{-1}) to label the energy axis. To obtain the energy value, one simply multiplies the velocity by a

constant $\frac{E_\gamma}{c}$, and for ^{57}Fe , $\frac{E_\gamma}{c} = 4.8075 \times 10^{-8} \text{ evmm}^{-1} \text{ s}$.

2.4.2 The Shape and Intensity of a Spectral Line

After a Mössbauer resonant absorption, the nuclear excited state is an isomeric state, which can only decay to the ground state through γ -ray emission or internal conversion. The cross-section of resonant absorption of γ -rays (as a function of photon energy E) is described by the Breit-Wigner formula :

$$\sigma_a(E) = \frac{\sigma_o \Gamma_a^2/4}{(E - E_o)^2 + \Gamma_a^2/4} \quad (2.11)$$

Where

$$\sigma_o = \frac{\lambda^2}{2\pi} \left(\frac{1+2I_e}{1+2I_g} \right) \frac{1}{1+\alpha} \quad (2.12)$$

is the maximum resonance cross-section, E_o and λ are the energy and wavelength of the γ -ray, I_e and I_g are, respectively, the nuclear spins of the excited and the ground states, and α is the internal conversion coefficient.

Because its excited state has a certain width Γ_s , the emitted γ -rays from the source are not completely monochromatic, but follow the Lorentzian distribution around E_o

$$\mathcal{L}(E) dE = \frac{\Gamma_s}{2\pi} \frac{1}{(E - E_o)^2 + \Gamma_s^2/4} dE \quad (2.13)$$

where

$$\int \mathcal{L}(E) dE = 1 \quad (2.14)$$

Therefore, in a situation where both the source and the absorber are very thin, the observed resonance absorption curve can be calculated by a convolution integral

$$\begin{aligned} \sigma_a^{\text{exp}}(E) &= \alpha \int \mathcal{L}(E-x) \sigma(x) dx \\ &= \frac{\sigma_o \Gamma_a}{\Gamma_a + \Gamma_s} \frac{\left(\frac{\Gamma_s + \Gamma_a}{2} \right)^2}{(E - E_o)^2 + \left(\frac{\Gamma_s + \Gamma_a}{2} \right)^2} \end{aligned} \quad (2.15)$$

and it is clear that the line shape is also Lorentzian, similar to Eq. (2.13) except that the line width becomes $\Gamma_s + \Gamma_a$. In reality, because of the finite thicknesses of the source and absorber, the emission and absorption spectral line widths Γ_s and Γ_a would be larger than the natural width Γ_n (for ^{57}Fe , $\Gamma_n \approx 0.097 \text{ mm s}^{-1}$), and the observed resonance line would be broader than $2\Gamma_n$.

We now discuss in detail how the thickness of an absorber influences the shape and intensity of a transmission spectrum. Let the total intensity of the γ – ray emitted by Mössbauer nuclei be I_0 , of which only a part I_r is recoil free and distributed according to a Lorentzian shape:

$$I_r(E, v, 0) = f_s I_0 \mathcal{L}\left(E - \frac{v}{c} E_0\right)$$

where f_s and v are the recoilless fraction and the Doppler velocity of the source. Going through the absorber, γ – ray intensity is reduced because of two absorption processes, a non-resonance atomic absorption (mainly the photoelectric effect) with a mass absorption coefficient of μ_a and a Mössbauer resonance absorption with an absorption coefficient of μ_r :

$$\mu_r = n_a f \sigma_a(E) \quad (2.16)$$

where n_a is the number of Mössbauer nuclei in the absorber per unit mass and f is the recoilless fraction of the absorber. Considering both of these absorption processes, the γ – ray intensity decreases exponentially after transmitting an absorber thickness d (mg cm^{-2}):

$$I_r(E, v, d) = f_o I_0 \mathcal{L}\left(E - \frac{v}{c} E_0\right) e^{-(\mu_a + \mu_r)d} \quad (2.17)$$

According to this, at a given Doppler velocity of the source, the intensity of the recoil-free γ – ray detected should be an integral over the energy:

$$I_r(v, d) = \int_{-\infty}^{+\infty} I_r(E, v, d) dE = f_s I_0 e^{-\mu_r d} T(v) \quad (2.18)$$

where

$$T(v) = \int_{-\infty}^{+\infty} \mathcal{L}\left(E - \frac{v}{c} E_o\right) A(E) dE \quad (2.19)$$

$$A(E) = \exp[-\mu_r(E)d] = \exp[-\sigma(E)t_a] \quad (2.20)$$

$$\sigma(E) = \sigma_a(E) / \sigma_o,$$

$$t_a = n_a f \sigma_o d \quad (2.21)$$

$T(v)$ is known as the transmission integral. As defined in Eq. (2.21), t_a is called the effective thickness of the absorber, and is temperature dependent in the same manner as f .

The rest of the γ – rays are emitted with recoil, and they are distributed in a rather broad energy range (Fig. 2.6) and absorbed solely due to the non-resonant absorption process. Thus, the intensity after absorption is independent of the Doppler velocity v and can be expressed as

$$I(d) = I_o(1 - f_s) e^{-\mu_a d} \quad (2.22)$$

Combining Eqs. (2.18) and (2.22), we obtain the total intensity recorded by the detector (whose efficiency is assumed to be 100%) as

$$I(v, d) = I_r(v, d) + I(d) = I(\infty, d) [1 - f_s + f_s T(v)] \quad (2.23)$$

where $I(\infty, d) = I_o \exp(-\mu_a d)$ is the spectral baseline corresponding to $v = \infty$.

If we neglect hyperfine interactions for the time being, the fractional intensity of the absorbed of γ – rays at a Doppler velocity v can be defined as

$$\varepsilon(v) = \frac{I(K, d) - I(v, d)}{I(K, d)} = f_s [1 - T(v)] \quad (2.24)$$

which describes the shape of the absorption spectrum. The fractional intensity $\varepsilon(v)$ can be obtained analytically and, at resonance $v = v_r = 0$, $\varepsilon(v)$ reaches its maximum

$$\frac{\varepsilon(v_r)}{f_s} = 1 - e^{-t_a/2} I_o(t_a/2) - 2 e^{-t_a/2} \sum_{n=1}^{\infty} \left(\frac{\xi - 1}{\xi + 1}\right)^n I_n(t_a/2) \quad (2.25)$$

which is explicitly expressed in terms of $\xi = \Gamma_s / \Gamma_a$. In the above equation, I_n is the modified Bessel function of the first kind of order n . If $\Gamma_n = \Gamma_a$, thus $\xi = 1$, Eq. (2.25) becomes

$$\varepsilon(v_r) = f_s [1 - e^{-t_a/2} I_0(t_a/2)] \quad (2.26)$$

which is a well-known result independent of both line widths. Next, we discuss the contribution of the third term in $\varepsilon(v_r)$, which will be abbreviated as ε_3 :

$$\varepsilon_3 = -2e^{-t_a/2} \sum_{n=1}^{\infty} \left(\frac{\xi-1}{\xi+1} \right)^n I_n(t_a/2) \quad (2.27)$$

The value of $\varepsilon(v_r)/f_s$ in Eq. (2.25) is plotted in Fig. 2.8 as a function of t_a and ξ . Regardless whether n is even or odd, $I_n(t_a/2)$ is always positive. Therefore, the sign of ε_3 is determined by the factor $(\xi-1)/(\xi+1)$. When $\xi < 1$, $\varepsilon_3 > 0$, and when $\xi > 1$, $\varepsilon_3 < 0$. The effect of this third term ε_3 is clearly demonstrated in Fig. 2.8. The curve with is completely consistent with those given.

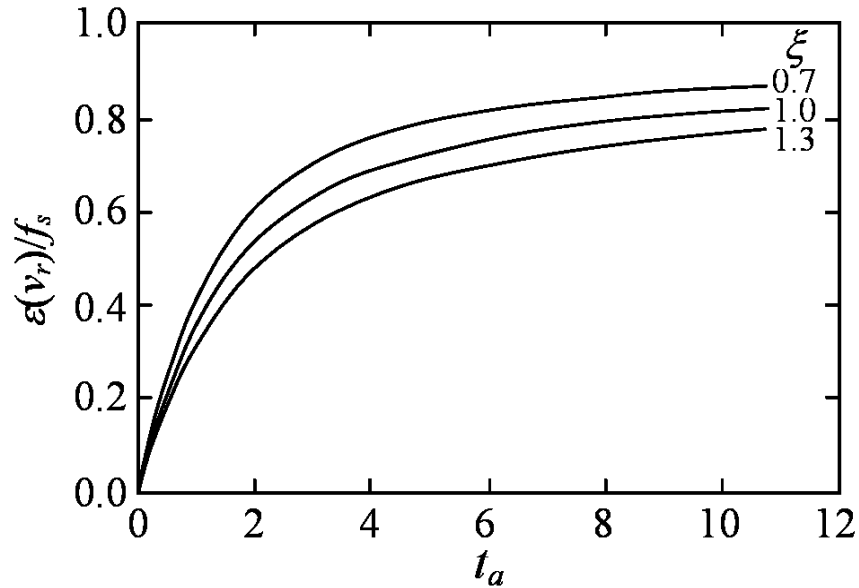


Fig. 2.8 $\varepsilon(v_r)/f_s$ as a function of t_a for $\xi = 0.7, 1.0, \text{ and } 1.3$.

In practice, cases with $\xi > 1$ are hardly observed and $\xi < 1$ is in the majority. Therefore, the influence of the third term on $\varepsilon(v_r)$ is essentially the addition of a

positive contribution. Obviously, when $t_a < 1$, such an influence becomes negligible regardless of the value of ξ .

In fact, the above argument can be understood in the following straightforward way. In the case where $\Gamma_s < \Gamma_a$ (or $\xi < 1$), the absorber in some sense looks like a “black absorber” absorbing the majority of resonant γ – rays. In other words, the resonant γ – rays, as a whole, have a higher probability of becoming absorbed.

Based on the above results, a transmission Mössbauer spectrum is sketched in Fig. 2.9 where I_b represents the background counts. During the above derivation, we assumed that the intensity was corrected by I_b . As long as the “thin absorber approximation” $t_a < 1$ is valid, one only need to take the first two terms in the polynomial expansion of $A(E)$ in Eq. (2.20). Then the fractional absorption intensity described in Eq. (2.24) can be easily written as:

$$\begin{aligned}
 \varepsilon(\nu) &= f_s [1 - T(\nu)] = f_s \int \mathcal{L}\left(E - \frac{\nu}{c} E_o\right) \left[1 - \exp\left(-\frac{t_a \sigma_o}{\sigma_o}\right)\right] dE \\
 &\approx f_s \int \mathcal{L}\left(E - \frac{\nu}{c} E_o\right) \frac{t_a (\Gamma_a/2)^2}{(E - E_o)^2 + (\Gamma_a/2)^2} dE \\
 &= \frac{\Gamma_a}{\Gamma_s + \Gamma_a} \frac{f_s t_a \left(\frac{\Gamma_s + \Gamma_a}{2}\right)^2}{\left(\frac{\nu}{c} E_o\right)^2 + \left(\frac{\Gamma_s + \Gamma_a}{2}\right)^2} \quad (2.28)
 \end{aligned}$$

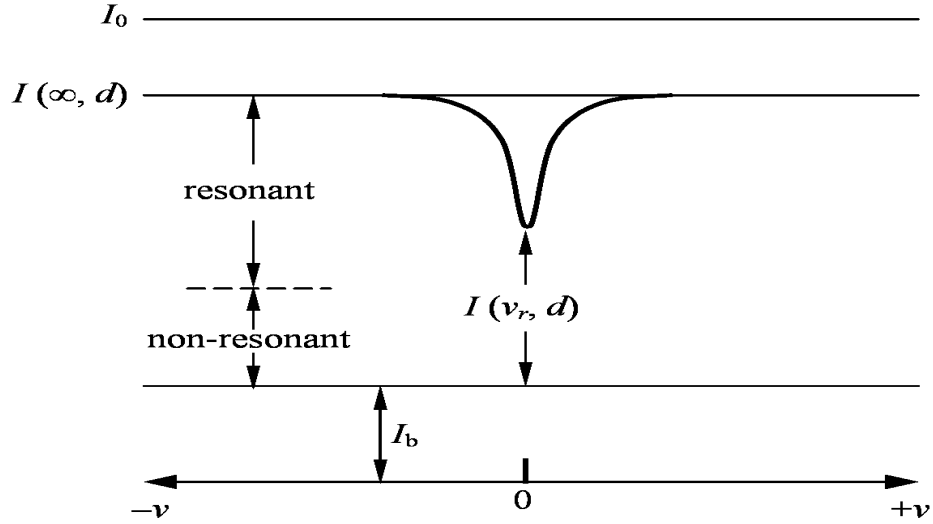


Fig 2.9. Contributions to the Mössbauer spectrum in transmission geometry.

This means when $t_a < 1$, the spectral shape is still Lorentzian. At resonance, expression (2.25) becomes identical to (2.28), only if $t_a < 1$ and $\Gamma_s = \Gamma_a$.

The area of absorption spectrum has been accurately calculated

$$A(t_a) = f_s \Gamma_a \pi \frac{t_a}{2} \exp\left(\frac{-t_a}{2}\right) \left[J_0\left(i \frac{t_a}{2}\right) + J_1\left(i \frac{t_a}{2}\right) \right] \quad (2.29)$$

where J_0 and J_1 are the zeroth- and first-order Bessel functions. Important parameters of a Mössbauer spectrum are the height, width, area, and position of a spectral line. Because of the constraint in Eq. (2.29), only two of the first three parameters are independent.

As the absorber thickness increases, the area $A(t_a)$, as well as $\varepsilon(\nu_r)$, deviates considerably from its linearity with t_a and gets saturated (see Figs. 2.10 and 2.8). Interpretation of Mössbauer spectra is often complicated by such a saturation effect due to a finite absorber thickness. A comparison between Figs. 2.10 and 2.8 shows how the area $A(t_a)$ saturates much less rapidly than $\varepsilon(\nu_r)$. A further analysis reveals that the spectral shape remains Lorentzian for up to $t_a \approx 10$.

Notice that $\varepsilon(\nu)$ describes the shape of the spectrum and obviously depends on both Γ_s and Γ_a , while the area $A(t_a)$ is an integral of $\varepsilon(\nu)$ over the Doppler velocity range (see Appendix A) and is only dependent on Γ_a .

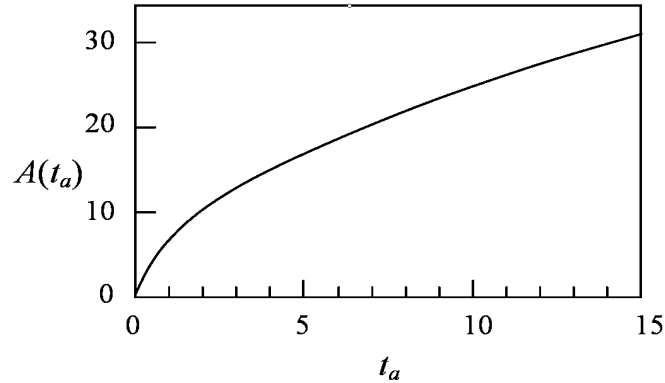


Fig. 2.10 $A(t_a)$ as a function of t_a . In plotting this curve, the proportionality constant $(f_s \Gamma_a \pi)$ in Eq. (2.29) is taken to be 1^{-2} .

2.5 Mössbauer isotopes

Several requirements can be formulated which must be fulfilled if there is to be an easily observable Mössbauer resonance :

1. The energy of the gamma ray must be between 10 and 150 KeV, preferably less than 50KeV, because the recoilless fraction f and resonant cross-section σ_0 both decrease as E_γ increases. This is the main reason why no resonances are known for isotopes lighter than ^{40}K . The γ -transitions in light nuclei are usually very energetic.

2. The half -life of the first excited state which determines Γ should be between about 1 and 100 n s. If $t_{1/2}$ is very long ,then Γ is so narrow that mechanical vibrations destroy the resonance condition, and if $t_{1/2}$ is very short, then Γ will probably be so broad as to obscure any useful hyperfine effects.

3. The internal conversion coefficient α should be small (<10) so that there is a good probability of detecting the γ -ray .

4. Along-lived precursor should exist which can populate the required excited level.

This usually means an isotope which decays by β -decay , electron capture ,or isomeric

transition. Although some experiments have been done with energetic nuclear reactions *in situ* such as coulombic excitation or (d,p) reactions, these methods are not applicable to routine measurements.

5. The ground -state isotope should be stable and have a high natural abundance so that isotopic enrichment of absorbers is unnecessary .

Despite these restrictions, a Mössbauer resonance has been recorded in 100 transitions of 83 different isotopes in 44 elements ,the majority of the heavy elements in fact. However , many of these resonances can only be recorded with difficulty at the present time .Some of the more useful resonances ,are listed in Table 2.2 .Some of their nuclear properties are also given ,including the nuclear spin states I_g and I_e and their parity ,and the internal conversion α .`

One of the most important experimental aspects is in the choice of a source matrix .It is very desirable to have a high recoilless fraction and a single emission line un broadened by hyperfine interactions. The best choice of host matrix is usually a high -melting metal or a refractory oxide of cubic structure, for example the most popular host for ^{119m}Sn is the oxide BaSnO_3 ,and ^{57}Co is usually diffused into a metal ,such as palladium,platinum or rhodium .However,these were chosen as the result of experience ,and the development of a good source is of prime importance in studying a new resonance .

In some instances where the absorption is too weak ,a substantial improvement can be obtained by using isotopic enrichment .Thus ^{57}Fe has an abundance of only 2.17% in natural iron, but material enriched to 90% can be used in compounds with a very low total iron content (e.g dilute iron alloys or haeme-proteins) to obtain an adequate cross-section for absorption ¹² .

| Isotope | $E_\gamma(\text{keV})$ | $\Gamma_\gamma(\text{mm s}^{-1})$ | I_g | I_e | α | Natural abundance | Nuclear decay* |
|-------------------|------------------------|-----------------------------------|-------|-------|------------|-------------------|---|
| ^{57}Fe | 14.41 | 0.19 | 1/2- | 3/2- | 8.17 | 2.17 | $^{57}\text{Co}(\text{EC } 270\text{d})$ |
| ^{61}Ni | 67.4 | 0.78 | 3/2- | 5/2- | 0.12 | 1.25 | $^{61}\text{Co}(\beta^- 99\text{m})$ |
| ^{99}Ru | 90 | 0.15 | 5/2 + | 3/2+ | - | 12.63 | $^{99}\text{Rh}(\text{EC } 16\text{d})$ |
| ^{119}Sn | 23.87 | 0.63 | 1/2+ | 3/2+ | 5.12 | 8.58 | $^{119\text{m}}\text{Sn}(\text{IT } 250\text{d})$ |
| ^{121}Sb | 37.15 | 2.1 | 5/2+ | 7/2+ | ~ 10 | 57.25 | $^{121\text{m}}\text{Sn}(\beta^- 76\text{y})$ |
| ^{125}Te | 35.48 | 5.02 | 1/2+ | 3/2+ | 12.7 | 6.99 | $^{125}\text{I}(\text{EC } 60\text{d})$ |
| ^{127}I | 57.6 | 2.54 | 5/2+ | 7/2+ | 3.7 | 100 | $^{127\text{m}}\text{Te}(\beta^- 109\text{d})$ |
| ^{129}I | 27.72 | 0.59 | 7/2+ | 5/2+ | 5.3 | nil | $^{129}\text{Te}(\beta^- 33\text{d})$ |
| ^{129}Xe | 39.58 | 6.85 | 1/2+ | 3/2+ | 11.8 | 26.44 | $^{129}\text{I}(\beta^- 1.7 \times 10^7\text{y})$ |
| ^{149}Sm | 22.5 | 1.6 | 7/2- | 5/2- | ~ 12 | 13.9 | $^{149}\text{Eu}(\text{EC } 106\text{d})$ |
| ^{151}Eu | 21.6 | 1.44 | 5/2+ | 7/2+ | 29 | 47.8 | $^{152}\text{Gd}(\text{EC } 120\text{d})$ |
| ^{161}Dy | 25.65 | 0.37 | 5/2+ | 5/2- | ~ 2.5 | 18.88 | $^{161}\text{Tb}(\beta^- 6.9\text{d})$ |
| ^{169}Tm | 8.4 | 9.3 | 1/2+ | 3/2+ | 220 | 100 | $^{169}\text{Er}(\beta^- 9.4\text{d})$ |
| ^{182}W | 100.1 | 2 | 0+ | 2+ | 3.2 | 26.4 | $^{182}\text{Ta}(\beta^- 115\text{d})$ |
| ^{189}Os | 69.59 | 2.41 | 3/2- | 5/2- | 8.2 | 16.1 | $^{189}\text{Ir}(\text{EC } 13.3\text{d})$ |
| ^{193}Ir | 73 | 0.6 | 3/2+ | 1/2+ | ~ 6 | 61.5 | $^{193}\text{Os}(\beta^- 31\text{h})$ |
| ^{197}Au | 77.34 | 1.87 | 3/2+ | 1/2+ | 4 | 100 | $^{197}\text{Pt}(\beta^- 18\text{h})$ |
| ^{237}Np | 59.54 | 0.067 | 5/2+ | 5/2- | 1.06 | nil | $^{241}\text{Am}(\alpha 458\text{y})$ |

Table 2.2 Nuclear parameters for selected Mössbauer transitions.

*EC=electron capture, β^- =beta-decay, IT=isomeric transition , α = alpha decay ¹²

2.6 Mössbauer parameters

The main Mössbauer parameters are summarized in Fig. 2.13.

The Mössbauer parameters are presented below in the simplest possible way. For a more detailed interpretation.

The chemical isomer shift δ_c is a parameter arising from the nuclear energy shift caused by the electric monopole interaction between the nucleus and the (s) electrons that have nonzero density at the site of the nucleus. Thus, the chemical isomer shift is influenced by the oxidation state and by the occupation numbers of electronic orbitals. A simplified formula implying this is as follows:

$$\delta_c = \Delta E_{IS} \frac{c}{E_0} = \alpha \Delta |\Psi(0)|^2 \quad (2.30)$$

where ΔE_{IS} is the difference between the median transition energies of the absorber (E_A) and the source (E_S) shown in Fig. 2.13, which is due to the fact that the Mössbauer nucleus is not naked, but sitting in the middle of well-determined atomic species both in the source and in the absorber; c/E_0 is the Doppler conversion factor from energy to speed (see eq.2.8); c is the speed of light in a vacuum; and $\Delta |\Psi(0)|^2$ is the difference between the electron densities at two identical nuclei, one of which is embedded in the source material, while the other in the absorber material*. The factor α comprises several factors including the relative difference between the nuclear radii of the excited state and the ground state for the same nucleus**. For small nuclei (e.g., ^{57}Fe and ^{119}Sn), α can be considered as being independent of the electron density, depending exclusively on the kind of the nucleus in question. Since the electron density may change from compound to compound (or, sometimes, from site to site), the chemical isomer shifts of different absorbers will be different even if they are measured with the same source (which is the usual thing to do).

**In general, the source is a standard and the absorber is the studied sample.*

***Therefore, it is important that the nuclear radius always changes on excitation, otherwise the isomer shift could not be observed at all.*

The second-order Doppler shift δ_{SOD} is related to the mean square speed' $\langle u^2 \rangle$ of lattice vibrations:

$$\delta_{\text{SOD}} = \Delta E_{\text{SOD}} \frac{c}{E_o} = \frac{-\langle u^2 \rangle}{2c^2} E_o \frac{c}{E_o} = \frac{-\langle u^2 \rangle}{2c} \quad (2.31)$$

where ΔE_{SOD} is the energy shift shown in Fig. 2.13. It follows from the above formula that δ_{SOD} decreases with the increase of temperature.

Isomer shifts δ , i.e., the peak shifts actually observed in Mössbauer spectra, consist of two terms:

$$\delta = \delta_c + \delta_{\text{SOD}} \quad (2.32)$$

where the first term is the chemical isomer shift δ_c , presented by eq. 2.30, which does not depend on the temperature, and the second term δ_{SOD} is the second-order Doppler shift discussed above. Since the latter is temperature-dependent (hence, the synonym temperature shift), the whole expression of δ is also temperature-dependent.

The quadrupole splitting Δ arises from the splitting of the nuclear energy levels caused by the inhomogeneous electric field of valence electrons and ligands. This interaction is determined by the nuclear quadrupole moment (Q) and the components E_{ij} of the **electric field gradient** (EFG) tensor caused by valence electrons and ligands at the nucleus. If the excited state is characterized by nuclear spin quantum number $I = 3/2$ and the ground state by $I = 1/2$ (which is the case with ^{57}Fe and ^{119}Sn), the quadrupole splitting is given by the formula:

$$\Delta = \Delta E_Q \frac{c}{E_o} = \frac{1}{2} eQV_{33} \sqrt{1 + \frac{\eta^2}{3}} \frac{c}{E_o} \quad (2.33)$$

where e is the elementary charge; ΔE_Q is the energy shift shown in Fig. 2.13 ; and η is the asymmetry parameter calculated from the second derivatives of the electric potential V

$$\eta = \frac{V_{11} - V_{22}}{V_{33}} \quad (2.34)$$

Note that the components of the EFG are obtained from the respective potential derivatives as follows:

$$E_{ij} = -V_{ij} = \frac{-\partial^2 V}{\partial x_i \partial x_j}$$

and therefore the V_{ij} s are often referred to (incorrectly) as the components of the EFG tensor. The coordinate axes x_1 , x_2 , and x_3 of the Cartesian system are labeled in such a way that:

$$|V_{33}| \geq |V_{22}| \geq |V_{11}|$$

For a point charge ez situated at $r = (x_1, x_2, x_3)$, the V_{ij} components at the nucleus ($r=0$)

$$\text{are as follows: } V_{ij} = ez \frac{3x_i x_j - r^2 \delta_{ij}}{r^3} \quad (2.35)$$

where δ_{ij} is the Kronecker symbol:

$$\delta_{ij} = \begin{cases} 1 & \text{for } i=j \\ 0 & \text{for } i \neq j \end{cases}$$

The quadrupole splitting is proportional to the peak separation of the corresponding **quadrupole doublet** (Fig. 2.13), and so it can be determined easily from the Mössbauer spectrum.

If ligand contribution is predominant in the quadrupole interaction, the individual ligands are usually considered as point charges whose effects are calculated from eq. 2.35. Summing up that equation, one can prove that the quadrupole splitting is zero for the cases of the highest symmetry in coordination and charge distribution (spherical, “ideal” hexahedral, octahedral, and tetrahedral). However, the often - cited statement that the lower the symmetry, the larger the quadrupole splitting is an oversimplification, which can lead to incorrect conclusions. (For instance, the ligand contribution of the EFG for an octahedral **trans FeA₂B₄** complex is twice that for the corresponding **cis**

configuration although the former one is obviously more symmetrical.)

The quadrupole splitting can also depend on the temperature (see the next section) owing to the temperature-dependent population of valence levels.

The magnetic splitting Δ_m observed in Mössbauer spectra arises from the Zeeman splitting of the energy levels of the nucleus provided that a nonzero magnetic flux density, B , exists there. The formula of Zeeman splitting is given as follows:

$$\Delta_m = \Delta E_m \frac{c}{E_0} = -g_I \mu_N B \Delta_{mI} \frac{c}{E_0} \quad (2.36)$$

where ΔE_m is the energy shift illustrated by Fig. 2.13 for the $I = 3/2 \rightarrow 1/2$ transition of ^{57}Fe (in the special case of $\Delta m_I = 1$); g_I is a nuclear factor that depends on the nuclear spin I of the nucleus; m_I is the magnetic quantum number; and μ_N is the nuclear magneton. It follows from the above formula that Δm has different values for the excited state (e) and for the ground state (g).

The magnetic flux density at the nucleus is proportional to the peak separation of the corresponding magnetic sextet (Fig. 2.11), and so it can be determined very easily from the Mössbauer spectrum.

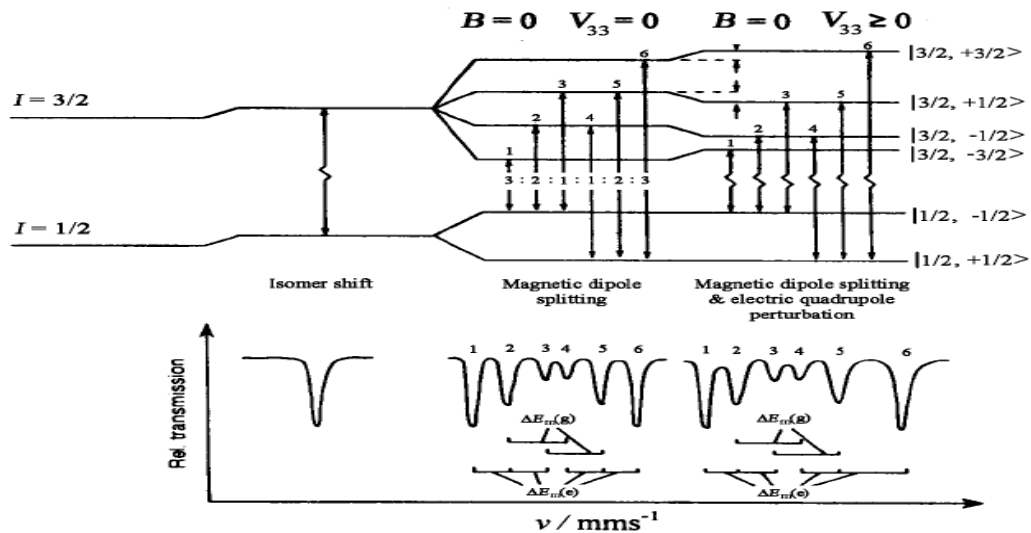


Fig. 2.11 Magnetic splitting with and without quadrupole interaction for ^{57}Fe . *

**The conventional unit of the (components of) isomer shift, quadrupole splitting, magnetic splitting, and peak width is mm/s in Mössbauer spectroscopy. The reason is as follows. When the spectrum is measured (see Fig. 2.11), the energy of the γ -ray is modulated via the Doppler effect. Since the Doppler speed of the source relative to the absorber is directly available, it is more convenient to scale the abscissa in speed unit than in energy. Note that the Doppler speed and the energy (shift) are in linear relationship with each other according to eq. 2.8.*

Magnetic splitting is not restricted to materials showing “actual” magnetism like ferromagnetic solids (e.g., α -Fe at room temperature) and ferrimagnetic ones (e.g., magnetite at room temperature). It can also be observed with antiferromagnetic crystals (e.g., with hematite or with MnO) in which the magnetic moments of the different sub lattices cancel each other, and thus they are not attracted by a magnet (see Fig.2.12). Even paramagnetic materials may produce magnetic splitting if the “flipping” of the unpaired spin is relatively slow for some reason.

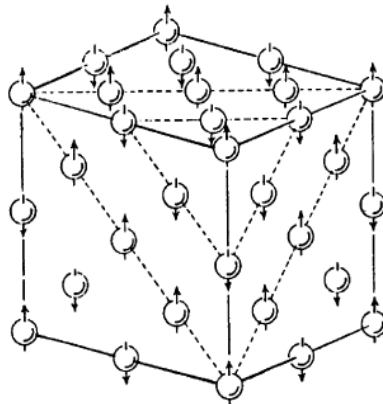


Fig. 2.12 The antiferromagnetic structure of MnO

The Mössbauer–Lamb factor f (also called, erroneously, the Debye–Waller factor) is a measure of the probability of recoil-free resonance fluorescence of γ – photons. It is defined as the number of recoil-free γ – events (emission or absorption) divided by the total number of γ events. It can be expressed by the following equation:

$$f = \exp\left(\frac{-4\pi^2\langle r^2 \rangle}{\lambda^2}\right) \quad (2.37)$$

where λ is the wavelength of the γ – radiation of the Mössbauer transition and $\langle r^2 \rangle$ is the mean-square amplitude of the vibration of the Mössbauer atom “frozen” in the lattice.

The Mössbauer–Lamb factor is one of the coefficients, that determine the Mössbauer peak area A as a function of the concentration of the atomic species which is reflected by that particular spectrum peak (or more generally, by the respective peak pattern discussed later). Since the relationship is monotonic (close to being proportional), the higher the concentration and the Mössbauer–Lamb factor of a given atomic species, the larger its share from the total spectrum area. In the thin-absorber approximation, e.g., for the peak area (intensity) A_k of the k^{th} Mössbauer atomic species, we have:

$$A_k \propto f_{a,k} c_{a,k} \quad (2.38)$$

where $f_{a,k}$ is the Mössbauer–Lamb factor of the k^{th} Mössbauer atomic species in the absorber and $c_{a,k}$ is the concentration of the same species in the absorber. A more general expression for the peak area is given by eq. 2.29.

The last Mössbauer parameter to be mentioned is **the experimental peak width W** (full width at half the maximum, **FWHM**) which dependence on temperature and absorber thickness ³.

| Parameter Formula | ⁵⁷ Fe energy level diagram with allowed transition Source (S) Absorber (A) | Schematic representation of absorption vs. relative speed of source and absorber |
|---|--|--|
| Chemical isomer shift $\delta_C \propto \Delta E_{IS} = \beta \Delta \psi(0) ^2$ | | |
| Second order Doppler shift $\delta_{SOD} \propto \Delta E_{SOD} = -\frac{\langle u^2 \rangle}{2c^2} E_0$ | | |
| Quadrupole splitting $\Delta \propto \Delta E_Q = \frac{1}{2} eQV_{33} \sqrt{1 + \frac{\eta^2}{3}}$ | | |
| Magnetic splitting $\Delta_m \propto \Delta E_m = -g_I \mu_N B$ | | |
| Peak width $W \geq W_0 \propto 2\Gamma = 2 \frac{\hbar \ln 2}{T_{1/2}}$ | | |

Fig . 2.13. Representation of the main mossbauer parameters for the $I=3/2 \rightarrow 1/2$ transition $E \approx E_\gamma$ is the median transition energy of the naked nucleus , Γ is the natural line width characteristic of both the emission and absorption profiles ,and W is the peak width ,The δ, Δ , and W values have speed unit (mm/s), E and Γ have energy unit ³.

2.7 Importance of Mössbauer's discovery

We have seen that when the emitting and absorbing atoms are embedded in a well-bound crystalline lattice then atoms are a definite probability for emission and absorption of gamma rays with out changing the phonon occupation number of the lattice .Under such circumstances,i.e during zero phonon processes the emitted gamma ray carries with it the full transition energy .Consequently Mössbauer effect is sometimes called zero phonon emission and absorption of gamma rays ,the recoilless emission and absorption of gamma rays ,or the resonance fluorescence of gamma rays. Much more important than the zero phonon emission or recoilless emission of gamma ray is the fact that the gamma ray emitted under conditions appropriate to Mössbauer effect has a natural line width determined entirely by the life time of the nucleus in the excited state .

Mössbauer effect was raised from a mere laboratory curiosity to an indispensable and valuable tool of a solid state physicists .With such sharp lines it is possible :

⌘ To observe and study a variety of hyperfine interactions such as

1. electrostatic monopole interaction between the nucleus and the **s electron** density at the nucleus.

2.electric quadrupole interaction between the quadrupole moment of the nucleus and the electric field gradient at the nucleus ,and

3.magnetic dipole interaction between the magnetic dipole moment of the nucleus and the magnetic field at the nucleus .

⌘ To observe gravitational red shift in a laboratory and test the equivalence principle .

Its investigations have led to various applications to diverse domains of science such as **nuclear physics, lattice dynamics ,coordination chemistry, biophysics**, etc ¹ .

CHAPTER 3

Some applications of Mössbauer effect

3.1 Mössbauer effect to General Relativity

One of the predictions of the general theory of relativity is the so-called red shift: that is, a clock or an atomic system that radiates energy of a definite frequency will have a longer period or emit a longer wavelength when in a strong gravitational field than it has in a weak field. The wavelength is thus shifted toward the red or longer wavelength end of the spectrum. The only verification of this prediction was the determination of the wavelength of light emitted from a very dense star. It occurred to several groups of physicists that the Mössbauer effect provided a means for checking this prediction by a terrestrial experiment.

It will be recalled that the intensity I_G of the gravitational field at a distance r from a large mass m is given by

$$I_G = \frac{GM}{r^2} \quad (3.1)$$

Where G is the universal constant of gravitation the intensity I_G , by definition is simply the force per unit mass at the given point. In the case of the earth's gravitational field.

$$I_G = g \quad (3.2)$$

The well known acceleration due to gravity. The gravitational potential Φ at the point r due to the mass M is simply.

$$\Phi = \frac{-GM}{r} \quad (3.3)$$

The concept involved in the terrestrial experiment is the equivalence between gravitational mass and inertial mass, a fact that has been verified to a high degree of accuracy by the experiment of EötVös. Another aspect of this concept is the equivalence of an accelerated system and gravitational field: that is, there is no way of distinguishing locally between the effects produced by gravitational field and an acceleration of a system in which an experiment is being performed. A system with an

acceleration a produces an effect equivalent to that of a gravitational acceleration $-g$ – the difference of potential between two points near the surface of the earth, one at a height H above other is, to a first approximation

$$\Delta \Phi = gH \text{ -----} \quad (3.4)$$

Where g is the average value of the gravitational acceleration over the height H . If the two points are close together near the surface of the earth, then $g = 980 \text{ cm/sec}^2$. To determine the difference in frequencies between two identical atomic (or nuclear) systems a distance H apart in gravitational field let us replace the latter with a system moving with an acceleration $a = -g$ but in a horizontal direction.

Figure 3.1 – shows a rigid rod of length H in an inertial frame of reference the rod is moving with a constant a to the right. Identical atoms (nuclei) are situated at the ends A and B of the rod. Suppose that at some particular instant when the velocity of the rod is v_1 the nucleus at A emits

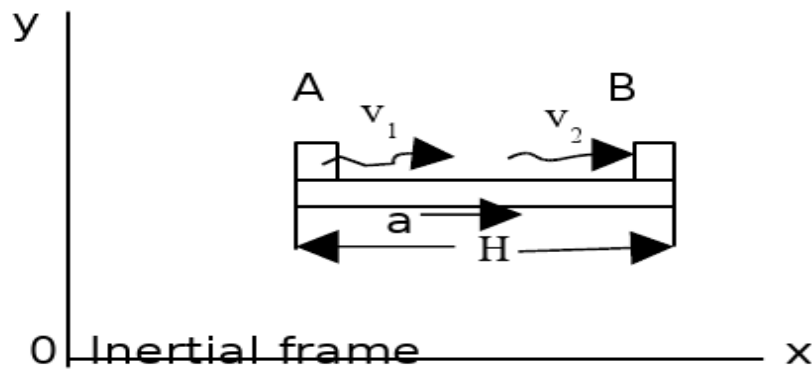


Fig.3.1. Rigid rod AB has constant acceleration a in inertial frame.

gamma-ray photon of frequency ν_1 in the direction of its motion. Because of its velocity v_1 at the instant of emission, the frequency as measured by a stationary observer will have been shifted by the Doppler effect to a value

$$\nu_{obs} = \nu_1 \left(1 + \frac{v_1}{c} \right) \quad (3.5)$$

This photon moves towards B with constant velocity c , and at a time

$$t = \frac{H}{c} \quad (3.6)$$

it will reach an identical nucleus that will act as the absorber .But the velocity v_2 of the rod and nucleus at this time is

$$v_2 = v_1 + at \quad (3.7)$$

The radiation that can be absorbed by B will have an apparent frequency ν_2 ,a stationary observer will report it as shifted by the Doppler effect to a value

$$\nu_{obs} = \nu_2 \left(1 + \frac{v_2}{c} \right) \quad (3.8)$$

For the identical gamma-ray photon to be the one emitted and absorbed we must have

$$\nu_1 \left(1 + \frac{v_1}{c} \right) = \nu_2 \left(1 + \frac{v_2}{c} \right) \quad (3.9)$$

The difference in frequency $\Delta \nu$ is therefore

$$\Delta \nu = \nu_1 - \nu_2 = \left(\frac{\nu_2 v_2 - \nu_1 v_1}{c} \right) \quad (3.10)$$

We can set $\nu = \nu_1 = \nu_2$ to a very good approximation and set

$$v_2 - v_1 = at = \frac{aH}{c} \quad (3.11)$$

So that

$$\Delta \nu = \frac{\nu aH}{c^2} \quad (3.12)$$

Thus in an accelerated system or ,from the principle of equivalence ,in a gravitation field in which the acceleration $g = -a$,identical atomic(nuclear)systems will emit or absorb radiation that will differ in frequency by an amount

$$\Delta \nu = \frac{\nu gH}{c^2} \quad (3.13)$$

Where H is the height of B above A . Stated another way, if $\Delta \Phi$ is the potential difference between two points in a gravitational field, the difference in frequency of identical clocks at these points will be ⁴

$$\Delta \nu = \frac{\nu \Delta \Phi}{c^2} \quad (3.14)$$

Let us now estimate the fractional change in frequency. By substituting the values of g and c^2 in equation (3.13), we find that the fractional change in the frequency will be approximately 1×10^{-16} per meter of height. This change is towards the lower-energy side and is called the gravitational red shift ¹.

3.1.1 Experiment

A series of experiments to verify this prediction was performed by R.V. Pound and G.A. Rebka, Jr., at Harvard (1959-1960) with ⁵⁷Fe as the emitter and absorber. A simplified schematic diagram of their apparatus is sketched in Fig. 3.2. The difference in height between A and B was 74 ft. The temperatures of the iron foils at A and B were measured accurately and corrections were made to the Doppler shift produced by the thermal motion of the crystal lattice.

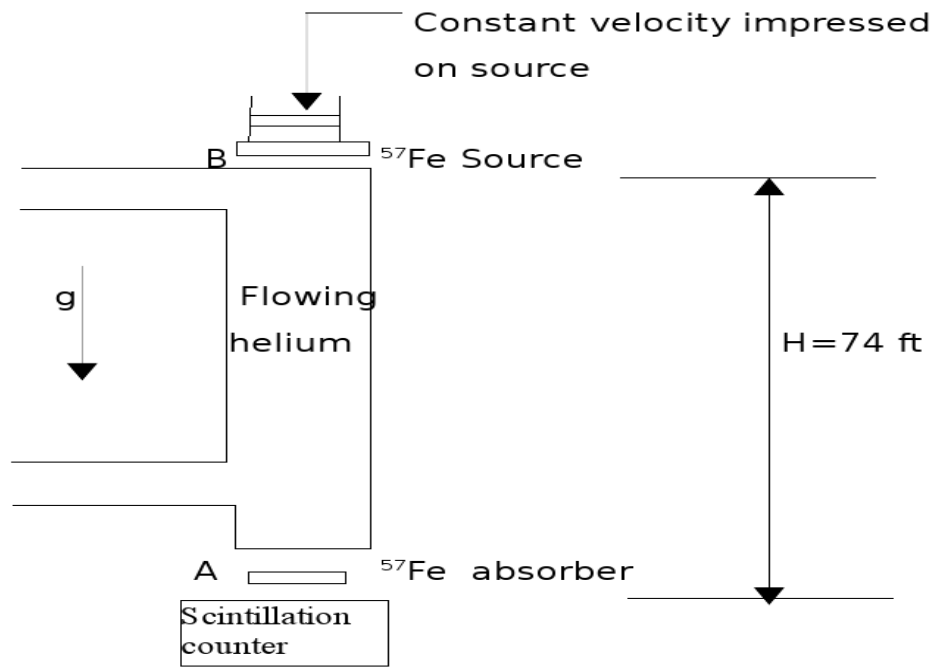


Fig 3.2. Simplified diagram of experimental arrangement for determining red shift.

A constant Velocity was impressed on the foil at B to provide the necessary Doppler shift to compensate for the gravitational red shift $\Delta\nu$ and to permit resonance absorption of the 14.4 –keV gamma ray from the source. A bag containing flowing helium was placed between the source and absorber to reduce the absorption of these photons that would occur in air. To improve the accuracy of the experiment the position of the absorber and source were interchanged ,thus providing abase line of $2H= 148\text{ft}$. The expected fractional frequency shift was

$$\frac{\Delta\nu}{\nu} = \frac{2gH}{c^2} = 4.92 \times 10^{-15} \quad (3.15)$$

The observed fractional frequency shift was 5.13×10^{-15} or ratio of 1.05 between the observed and theoretically shift . The frequency increased in falling , as expected . There is thus good agreement between theory and experiment ⁴.

3.2 Mössbauer effect in Dy₂O₂S

3.2.1 Introduction

In this work the recoilless absorption spectra of the 26 keV gamma rays from ¹⁶¹Dy situated in Dy₂O₂S have been recorded at various temperatures. This compound belongs to the family of rare earth oxisulfides T₂O₂S, which is of increasing interest.

The crystal structure can be described in the space group P3m (D₃³d) with 2 T in $\pm (\frac{1}{3}, \frac{2}{3}, u)$ ($u \simeq 0.3$), 2 O in $\pm (\frac{1}{3}, \frac{2}{3}, v)$ ($v \simeq 0.6$) and 1 S in (0, 0, 0); the point group of Dy³⁺ is C_{3v}. The susceptibility measurement shows that 1/χ versus T varies linearly with a Curie constant equal to that of the free ion, so that the overall splitting of the ground multiplet is of the order of a few tenth of Kelvins; the first excited multiplet lies far above it. The magnetic cell of Dy₂O₂S has been found by neutron diffraction to correspond to the propagation vector $k = [0, \frac{1}{2}, \frac{1}{2}]$.

The motivation of this study lies in the discrepancy between the values of the magnetic moment, as determined by neutron diffraction at 1.5°K (4.41 μ_B) and magnetization measurements (8.6 μ_B at 1.13 °K)

3.2.2 Experiment and conclusion

1. GYROMAGNETIC RATIO. - As it is well known, the hyperfine interactions measured by Mössbauer effect or other techniques, involve the product of two quantities, one of nuclear origin and the other of electronic origin. Therefore as far as solid state physics is concerned, one must know accurately the nuclear moments.

From a computer fit of our experimental results on Dy₂O₂S, (Fig. 3.5 d) we derive the ratio for magnetic moments:

$$\frac{\mu_e(26 \text{ keV})}{\mu_g} = -1.243 \pm 0.010$$

and the ratio for the electric quadrupole moments:

$$\frac{Q_e}{Q_g} = 1.007 \pm 0.010$$

These values are in complete agreement with those of Bowden et,al with a some what better precision. The discrepancy with other authors probably lies in the problem of the linearity of the drive system.

2. MAGNETIC STRUCTURE DETERMINATION

In figure 3.3 we represent the crystallographic and magnetic

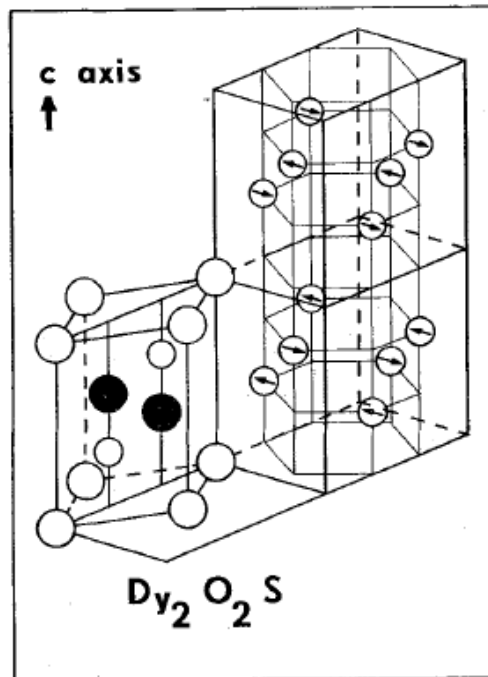


Fig. 3.3. -Magnetic structure of Dy_2O_2S as determined by neutron diffraction measurements.

structures of Dy_2O_2S , determined by neutron diffraction ; the magnetic ordering consists of an anti-ferromagnetic collinear arrangement, but some uncertainty exists because of the measured very low magnetic moment. From the comparison of the Mössbauer spectra : taken at $1.5^\circ K$ for the single crystal and powder sample respectively (Fig. 3.4 and Fig. 3.5a), we see that there are less lines in figure 3.4 where only 10 lines are present. The $\Delta m=0$ lines have vanished. From this observation we immediately conclude that the hyper fine magnetic field is directed along the c-axis, thus demonstrating that (within $\pm 5^\circ$):

1. the magnetic moments are indeed collinear,
2. their direction is not perpendicular but parallel to the c-axis, contrary to the neutron diffraction results.

Of course, because of its local nature, a hyperfine measurement cannot distinguish the relative orientation of next neighbour magnetic moments ; neutron diffraction measurements are under way in our laboratory, to elucidate this point.

The **experimental parameters are given in the following table :**

| | $\overline{g_g \mu_p H_{eff}}$ (MC/s) | $\overline{e^2 qQ}$ (MC/s) | $\overline{\mu_{4f}}$ (μ_B) |
|--------|--|-------------------------------|--------------------------------------|
| 4.2 °K | - (690 ± 20) | - 2 020 ± 50 | (8.0 ± 0.3) |

The quadrupole interaction is fairly large, and y is supposed to be zero since the c-axis is a three fold axis.

The hyperfine interaction seems to remain constant with an increase of the temperature, so that we get for the magnetic moment of the 4f shell the saturation value ; we have $\mu = (8.0 \pm 0.3) \mu_B$, showing that crystalline field effects are important in this compound.

The spectra of the Dy₂O₂S polycrystalline sample show that relaxation takes place ; even at 1.5 °K the central peak is greater than expected from the computed spectrum, and its intensity grows with the temperature together with a broadening of the lines, and eventually only the central peak is observed at about 6 °K.

The broadening of the lines takes place between 5°K and 6 °K i. e. at temperatures corresponding to the Neel temperature found by neutron diffraction (T = 5.8 °K).

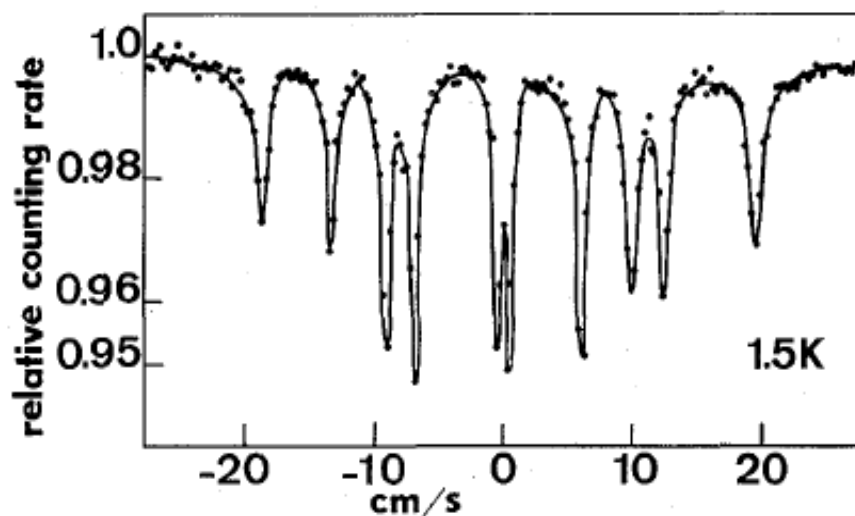


Fig.3.4 .Mössbauer spectrum of Dy_2O_2S single crystal,exhibiting the disappearance of the $\Delta m=0$ lines.

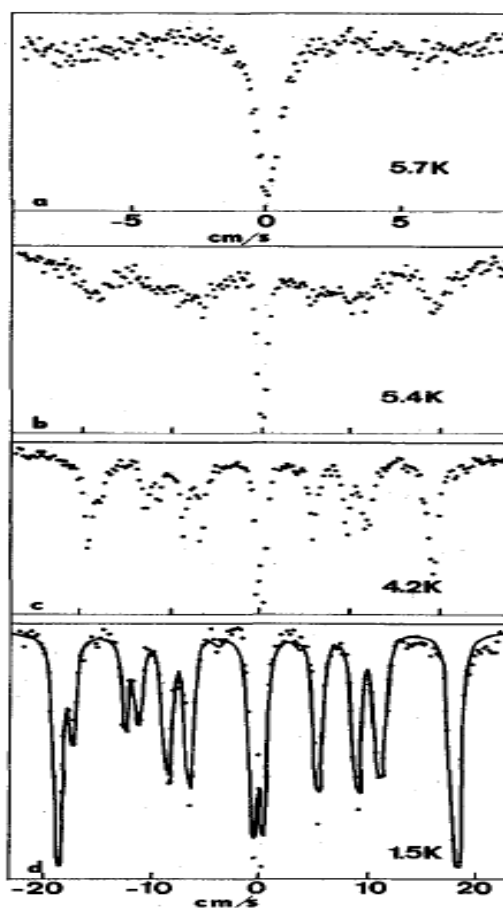


Fig. 3.5a,b ,c ,d-Mössbauer spectra of Dy_2O_2S power sample at different temperatures:Figure 3.5d is a computer fit.

Conclusion. - This study is a clear example of the usefulness of the Mössbauer effect technique for the study of magnetic structure, especially when single crystals are available. The determination of the absolute value of the magnetic moment can be reached within a few percent, as well as its direction.

These results are interesting especially for neutrons highly absorbing substances when the neutron diffraction results are difficult to interpret, and always less accurate ; more typically, experiments with single crystal of Gd compounds using the ^{161}Dy (26 keV) γ — rays could give direct information on the magnetic moment direction of the Gd ion⁵ .

CONCLUSION

Nuclear resonance scattering is the kinds of interaction with nucleons and its effect is Inelastic scattering (incoherent). This type of scattering involves the excitation of a nuclear level by an incident photon ,with subsequent reemission of excitation energy .After many unsuccessful searches ,suitable conditions appear to have been found for production a Doppler broadened emission line which is wide enough to overlap the scattering resonance and thus permit detection of nuclear resonance scattering ⁶ .

Mössbauer effect : emission or absorption of a gamma photon with out energy loss (or gain) in a transition between the ground state and an excited state of certain nuclei bound in a solid ⁷ .

SUMMARY OF OBSERVED RECOILLESS GAMMA TRANSITION [11]

| E_γ keV* | Resonant isotope | $T_{1/2}$ sec† | Γ/E_γ ‡ |
|--------------------|---------------------|-----------------------|---------------------|
| 8.4 | Tm ¹⁶⁹ | 8.0×10^{-9} | 7×10^{-12} |
| 14.4 | Fe ⁵⁷ | 1.0×10^{-7} | 3×10^{-13} |
| 24 | Sn ¹¹⁹ | 1.8×10^{-8} | 1×10^{-12} |
| 26 | Dy ¹⁶¹ | 2.8×10^{-8} | 6×10^{-13} |
| 27 | I ¹²⁹ | | |
| 71 | Ni ⁶¹ | 5.3×10^{-9} | 1×10^{-12} |
| 73 | Ir ¹⁹³ | 5.7×10^{-9} | 1×10^{-12} |
| 77 | Au ¹⁹⁷ | 1.9×10^{-9} | 3×10^{-12} |
| 80 | Er ¹⁶⁶ | 1.8×10^{-9} | 3×10^{-12} |
| 84 | Y ¹⁷⁰ | 1.6×10^{-9} | 3×10^{-12} |
| 87 | Gd ¹⁵⁵ | | |
| 93 | Zn ⁶⁷ | 9.4×10^{-6} | 5×10^{-10} |
| 100 | W ¹⁸² | 1.3×10^{-9} | 4×10^{-12} |
| 113 | Hf ¹⁷⁷ | 4.0×10^{-10} | 1×10^{-11} |
| 129 | Ir ¹⁹¹ | 1.3×10^{-10} | 3×10^{-11} |
| 134 | Re ¹⁸⁷ | 1.1×10^{-11} | 3×10^{-10} |

* Gamma-ray energy.

† Half life of excited state.

‡ Γ is the natural line-width.

A nucleus can absorb only that gamma ray photon whose energy is equal, within the limits set by the uncertainty principle ,to the difference in energy between an excited state and the ground state of the nucleus .In other words the absorbing nuclei must be

identical to the emitting ones .This is what we have termed as the resonance absorption .Clearly ,it will occur only when the emission of the gamma ray is recoilless, otherwise the gamma ray energy is reduced so much that it cannot resonate with a nucleus of the same kind ⁸ .

If the natural width Γ of the excited level is more than ΔE_R ,the resonance absorption is possible .On the other hand if the width Γ is less than ΔE_R ,resonance absorption is not possible.

According to the uncertainty principle ,for an excited energy level of with $\Delta E = \Gamma$ and life time $\Delta t = \tau$,we get $\Gamma\tau \geq \hbar$. In the case of atomic transitions,the mean life time τ of an excited level is 10^{-8} sec. Therefore the width of the level is $\Gamma \sim \hbar / \tau \approx 10^{-7}$ eV. The photons emitted have energies of the order of an electron volt, say $h\nu = 1\text{eV}$. For an atom of $A=100, Mc^2 \approx 10^{11}\text{eV}$. Thus $\Delta E_R \approx (1\text{eV})^2 / 10^{11}\text{eV} = 10^{-11}\text{eV}$ that is , $\Delta E_R \ll \Gamma$. Hence,resonance absorption is always possible in atomic transitions.

On the other hand,in the nuclear decay , $h\nu$ is approximately $100 \text{ KeV} = 10^5 \text{ eV}$.While Mc^2 is still 10^{11}eV (for $A=100$) Thus $\Delta E_R = (10^5\text{eV})^2 / 10^{11}\text{eV} = 10^{-1}$,Which is greater than the natural widths $\Gamma = 10^{-4} \text{ eV}$ of the nuclear levels.

Let us say that , in atomic systems $\Gamma / \Delta E_R \approx 10^3$, while in the nuclear systems $\Gamma / \Delta E_R \approx 10^{-3}$.This means that resonance absorption is possible in atomic systems, but not always in nuclear ones.

There are two different ways of achieving resonance absorption for high energy or nuclear transitions

1.one is to increase the width of the levels by some means so that the condition that $\Gamma > \Delta E_R$ is satisfied,which can be achieved by Doppler broadening .

This use of Doppler effect increased the frequency of the emitted radiation enough to compensate for the loss of energy due to recoil .

2.The other method is to reduce the loss of energy due to recoil so that ΔE_R is less than Γ . This accomplished by the Mössbauer effect. Which reduces the atom's energy

loss due to recoil almost to zero ⁹ .

Doppler-broadened lines obtained by the following means-

(a) By mounting a radioactive source on the tip of a high -speed rotor and using the Doppler effect to increase the frequency of the emitted radiation. The speed required is given by

$$E\gamma(v/c) = (E\gamma)^2/Mc^2$$

and for a nucleus of mass 200 and $E\gamma=500\text{KeV}$ the value $v=820\text{m/s}$ is found.

(b) By heating the radioactive source so that the Doppler phonon broadening is largely increased .The temperature of up to 1500K have been used.

(c) By utilizing a preceding transition ,such as β -decay, gamma decay or production in a nuclear reaction to provide the necessary velocity for Doppler shift of frequency ¹⁰ .

REFERENCES

- [1]. V.G.BHID, Mössbauer effect and its applications, TataMcGraw-Hill, New Delhi, 1973
- [2]. Yi-Long Chen and De-ping Yang, Mössbauer effect in lattice Dynamics, copy right ©2007 WILEY-VCH Verlag GmbH and co.KGae, Weinheim ISBN:978-3-527-40712-5
- [3]. E.KUZMANN, S. NAGY , AND A. VERTES, pure appl.chem, vol.75, No.6. pp.801-858, 2003 © 2003 IUPAC
- [4]. H. SEMAT AND J.R .ALBRIGHT, Introduction to atomic and Nuclear physics 5th edition ,London CHAPMAN AND HALL, 1973
- [5]. M.BELAKHOVSKY, centre d' Etudes Nucleaires ,38 ,Grenoble ,France ,Juurnal DE PHYSIQUE Colloque cl ,Supplement au no 2-3 ,Tome 32 , Fevrier- mars 1971 pp. cl- 915
- [6]. ROLEY D. EVANS, ph.D.(Proffessor of physics) ,The atomic Nucleus , 1955
- [7]. M. Darby Dyar, Mössbauer spectroscopy of Earth ,and planetary Materials, Annu.Rev.Earth planet .Sci. 2006.34:83 – 125
- [8]. S. B. PATEL, Nuclear physics An introduction ,1991
- [9]. ARAYA, A. Elementary Modern physics , 1974
- [10]. W. E. BURCHAM F.R.S , Elements of Nuclear physics , New York and London , 1979
- [11]. R. L. MÖSSBAÜER, Recoilless Nuclear resonance absorption , Ann. Rev. Nucl. Sci. 1962 .12: 123 - 152
- [12]. T.C . GIBB , Principles of Mössbauer spectroscopy , CHAPMAN AND HALL .LONDON ,1976